Particle & Particle Systems Characterization
www.particle-journal.com

Microfluidic Templating and Initiator-Free Photocrosslinking of Protein-Loaded PCL Microcapsules

*Florian Störmann, Toralf Roch, Andreas Lendlein, and Christian Wischke**

Polymer network materials are interesting alternatives to thermoplastic polymers. Here, the preparation of polymer capsules is investigated, which are made from poly(ϵ-caprolactone) (PCL) networks and are compartmentalized in a crosslinked PCL shell and a core that is suitable to enclose payloads of interest. Aided by microfluidic templating, PCL network capsules with a narrow size distribution (176 ± 5 µm) and thin shells (≈7.5 µm) are formed from 4-arm star-shaped 12 kDa PCL precursors by photoinitiator-free UV light-induced radical polymerization of methacrylate end-groups. FITC-BSA is encapsulated as a model protein. The physicochemical characterization of the capsules indicated a partial crosslinking of methacrylate endgroups into netpoints. Microscopy revealed a fraction of collapsed capsules that are discussed in the context of network stability and mechanical stress created at the capsule interfaces during solvent removal. The incubation of particles with human embryonic kidney (HEK) cells showed good cell compatibility, suggesting their potential use in biosciences and beyond.

1. Introduction

Polymer network materials[1] have become a cornerstone in various fields of application. Their usage expands from consumer products like mattresses and tires to high value products like tissue engineering scaffolds, hydrogels for drug delivery,[2] and cutting edge technologies like soft actuators.[3,4] For these applications, sets of specific material properties are needed to be tunable to the respective needs. Examples of characteristic features of network materials include tunable mechanics,[5–8] altered degradation pattern,[9,10] mesh size-dependent diffusivity of solutes,[11,12] or preserved integrity of outer shapes at elevated temperatures, where non-crosslinked equivalents would become a molten fluid. In the field of life sciences, polyester-based networks have been explored as degradable functional materials.[13–15]

A polyester of specific interest for this study is poly(ϵ-caprolactone) (PCL), which has a track record (as non-crosslinked material) in particulate carrier systems.[16–18] PCL has also been crosslinked to macroscopic networks, e.g. via methacrylate chemistry,[19] as well as to monolithic particles.[20,21] This can be a motivation to explore PCL-based network materials also for substructured particles. More specifically, the introduction of an aqueous core into the particles opens up the possibility to host water-soluble substances, e.g., for particle visualization, sorting, compound transportation, or drug delivery purposes. In all these cases, the aqueous core should be well defined in size to control the loaded volume of the payload.

In order to facilitate PCL crosslinking to networks, highly reactive initiators have been employed to speed up the thermosetting process.[19,22] This thermosetting is typically conducted at elevated temperatures up to 150 °C and, thus, is hardly compatible with particle preparation procedures in aqueous dispersion. As an alternative, the crosslinking of PCL-methacrylate in a photoreaction[23,24] appears more suitable for the desired capsule formation. While photoinitiators can accelerate the crosslinking reaction, they could undesirably diffuse in two-phase systems (particles, suspension medium) and thus get lost from the polymer phase. Remaining photoinitiators can potentially be toxic, which must be excluded when aiming at life science applications. Therefore, the use of photoinitiators may not be desirable here. The reaction conditions for photocrosslinking are other important parameters for consideration. It was shown before that the photocrosslinking of PCL particles in solid-state leads to network inhomogeneities that are disadvantageous.[20] In contrast, an excellent structure of monolithic PCL particles was observed when being crosslinked in solution state.[21] However, capsule preparation by crosslinking in solution will be more challenging due to the need to preserve the double emulsion to be stable for extended periods under photocrosslinking conditions. For macroscopic samples, the methacrylate-based photocrosslinking of PCL in the absence of a photoinitator was shown to proceed without major photodamage of the polyester,[25] which motivated the application of this methodology in the current study.

F. Störmann, T. Roch, A. Lendlein, C. Wischke[+]
Institute of Active Polymers
Helmholtz-Zentrum Hereon
Kantstraße 55, 14513 Teltow, Germany
E-mail: christian.wischke@pharmazie.uni-halle.de;
christian.wischke@hereon.de

The ORCID identification number(s) for the author(s) of this article can be found under https://doi.org/10.1002/ppsc.202300099

[+]Present address: Current address: Institute of Pharmacy, Martin-Luther University Halle-Wittenberg, Halle Germany

DOI: 10.1002/ppsc.202300099

In order to prepare double emulsion droplets as particle templates, microfluidic droplet templating can provide beneficial control of the particle morphology, sizes and loading efficiency.[26] By this method, the particles are formed drop per drop at the rendezvous of the different fluid phases inside a microfluidic device, thereby providing a well-defined process with negligible droplet size deviations. Such mild dispersion processes may be advantageous for the handling of delicate payloads like proteins, which in many cases are sensitive to shear forces during encapsulation.[27,28] In fact, the use of microfluidics for the preparation of polymer particles has received increasing attention, e.g. some literature reports are available describing the microfluidic preparation of non-crosslinked monolithic PCL particles[29,30] and PCL capsules.[31] As summarized in recent reviews (e.g., ref. [32]), also polymerization reactions have been used to stabilize capsules from various materials after microfluidic templating, while the preparation of PCL network capsules has not yet been established by this technique according to the authors knowledge.

In this study, the production of homogeneously sized PCL-network core-shell particles should be explored using a dye-labeled model protein as exemplary payload and microfluidic double-emulsification as a templating technique. For providing maximum loading, a thin capsule shell was envisioned, which should be stabilized by crosslinking of methacrylate chain terminations of oligomeric ϵ-caprolactone (oCL) precursors. Poloxamer 407, as previously identified to support protein stability,[33] was added to the inner aqueous phase, Span 80 was supplemented to the organic polymer solution, and polyvinyl alcohol (PVA) was employed in the outer aqueous phase for stabilizing the polymer-phase droplets against coalescence. The polymer network formation, capsule sizes and integrity, protein encapsulation, and the cell compatibility of the carriers was studied in vitro.

2. Experimental Section

2.1. Materials

Pentaerythritol (PERT) was obtained from Alfa-Aesar (Karlsruhe, Germany) and sublimated at 200 °C under high-vacuum before usage. ϵ-Caprolactone (CL) and calcium hydride (CaH_2) were obtained from Acros (Geel, Belgium). CL was dried over CaH_2 under permanent stirring for 24 h, was then distilled at 3 mbar at a head-temperature of 77 °C, and subsequently stored over molecular sieve 3A. Dichloromethane (DCM) was received from JTBaker (Deventer, Netherlands) and dried for at least 24 h over molecular sieve 3A. Sorbitan monooleate (Span 80), 2-isocyanatoethyl methacrylate (IEMA), toluene, fluorescein isothiocyanate-conjugated bovine serum albumin (FITC-BSA), tin(II) 2-ethylhexanoate, dibutyl tin(II)-dilaurate (DBTL), Poloxamer 407 (polyethylene glycol (PEG)/polypropylene glycol (PPG) triblock-copolymer PEG-*b*-PPG-*b*-PEG with a weight-average molecular weight M_w of ≈ 12500 g mol^{-1} and a PEG weight fraction of 0.7), fluorescein diacetate (FDA) and propidium iodide (PI) were all obtained from Sigma–Aldrich (Taufkirchen, Germany). Chloroform ($CHCl_3$), diethyl ether (Et_2O), methanol (MeOH), molecular sieve 3A and sodium chloride (NaCl) were purchased from Merck (Darmstadt, Germany). Polyvinyl alcohol (PVA, Mowiol 4-88) with M_w ≈ 31 000 g mol^{-1} was kindly provided by Kuraray (Hattersheim am Main, Germany). Octadecyl trimethoxysilane was purchased from Fluorochem, 2-[methoxy(polyethyleneoxy) propyl]trimethoxysilane (6–9 PEG repeating units) was delivered from ABCR (both from Karlsruhe, Germany). All other chemicals were used as received. Deionized water in Milli-Q quality was used throughout the experiments.

2.2. Synthesis of Oligomers

2.2.1. Star-Shaped Oligo(ϵ-caprolactone) (soCL-OH) Precursors

All glassware was dried three times by heating up to 500 °C with subsequent evacuation and argon purging. CL (78.92 g, 691 mmol) and PERT (1.36 g, 10 mmol) were added into a 250 mL round flask and heated to 135 °C under constant stirring. After complete dissolution of PERT in CL, catalytic amounts of tin(II) 2-ethylhexanoate (0.06 mL, 0.2 mmol) were added. The polymerization was stopped after 24 h by cooling to room temperature and dissolution of the white, waxy solid in DCM (150 mL). The dissolved soCL-OH was then precipitated in the tenfold amount of ice-cold methanol, filtered and washed several times with ice-cold methanol. The obtained white solid was then dried at 40 °C and high vacuum (< 1 mbar) for 4 h. The obtained yield was 97 mol%.

^{1}H-NMR (500 MHz, $CDCl_3$) δ [ppm] = 4.12 (8H, s), 4.06 (200H, t), 3.65 (7H, m), 2.31 (208H, t), 1.65 (416H, m), 1.39 (208H, m).

^{13}C-NMR (125 MHz, CDCl3) δ [ppm] = 173.5 (C_1), 64.1 (C_6), 34.1 (C_2), 28.3 (C_5), 25.5 (C_4), 24.6 (C_3).

2.2.2. IEMA-Functionalization of the soCL-OH Precursors

soCL-OH (75.03 g, 6.5 mmol) was dissolved in dry DCM (450 mL) in a previously dried 500 mL round flask. After the addition of 4.9 equivalents of IEMA (4.5 mL, 31.8 mmol) under constant stirring, catalytic amounts of DBTL (0.05 mL, 0.07 mmol) were added. The reaction vessel was sealed under argon for 5 days and stirred at room temperature. The reaction system was then precipitated in the tenfold amount of ice-cold Et_2O, filtered, and washed with ice-cold Et_2O. After drying at 40 °C and high vacuum for 4 h, a white solid (soCL-IEMA) was obtained (yield ≈ 100 mol%).

^{1}H-NMR (500 MHz, $CDCl_3$) δ [ppm] = 6.07 (3.4H, m), 5.54 (3.4H, bs), 5.07 (2H, m), 4.17 (8H, m), 4.05 (8H, s), 4.01 (152H, t), 3.44 (8H, m), 2.25 (144H, t), 1.89 (8H, s), 1.60 (288H, m), 1.33 (144H, m).

^{13}C-NMR (125 MHz, CDCl3) δ [ppm] = 173.3 (C_1), 167.1 (M_5), 156.47 (M_1), 135.8 (M_6), 125.8 (M_7), 64.6 (M_4), 64.0 (C_6), 63.6 (I_2), 39.9 (M_3), 33.9 (C_2), 28.2 (C_5), 25.4 (C_4), 24.4 (C_3), 18.1 (M_{10}).

2.3. Microfluidic Device Fabrication, Microcapsule Templating, and Crosslinking

The formation of double-emulsion templates was performed in microfluidic glass capillary devices with focused-flow geometry.

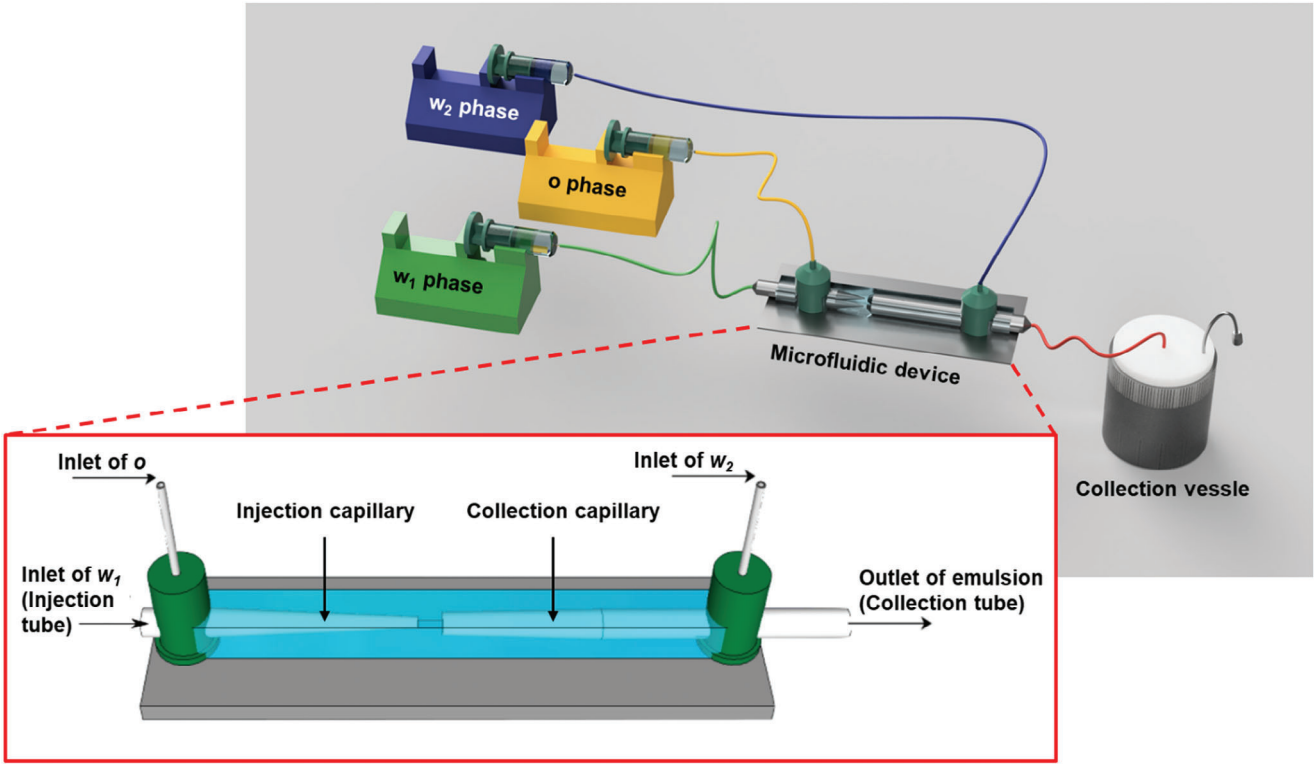

Figure 1. Scheme of glass-capillary microfluidic device for templating of PCL network capsules.

A square capillary of 1 mm inner diameter was used to insert two round capillaries (outer diameter: 1 mm). The round injection capillary (IC), which transports the inner aqueous phase (10 wt% Poloxamer 407, 100 µg mL^{-1} FITC-BSA, 1.8% (m/V) NaCl) was tapered to an orifice diameter of 50 µm and silanized with octadecyl trimethoxysilane. The round collection capillary (CC), responsible for the transport of the generated double-emulsion droplets, was tapered to an orifice diameter of 360 µm and silanized with 2-[methoxy(polyethyleneoxy) propyl]trimethoxysilane. The two inlets of the square capillary were capped by blunt cannulas and fixed by epoxy glue. The middle phase (8.2 wt% soCL-IEMA, toluene/chloroform with a volume fraction φ_i of 0.742/0.258, 1.6 wt.% Span 80) was transported through the square capillary from the same side as the IC, while the aqueous continuous phase (5 wt% PVA, 1.8% (m/V) NaCl) was fed from the opposite side into the square capillary. The free end of the CC was connected to a tubing for sample collection (**Figure 1**).

The double-emulsion droplets were produced at flow-rates of $w_i/o/w_o$ = 0.4/2.0/14.0 mL·h^{-1} and were harvested in an isotonic aqueous collection bath (1.8% (m/V) NaCl, chloroform saturated). Subsequently, the droplets were irradiated for 8 min by a XeCl-excimer light source (Bluelight, Heraeus, Hanau, Germany, 308 nm, 5 cm distance, 69% output, 3.0 Ampere). Then, the organic solvent was slowly extracted and evaporated from the aqueous phase over night at the air interface. The capsule suspension was then dialyzed against an isotonic aqueous solution (1.8% (m/V) NaCl) for two days for removing leachable such as excess PVA from the continuous phase.

2.4. Characterization Methods

^{1}H and ^{13}C-NMR analyses of the oligomeric precursor were performed on a 500 MHz spectrometer (Avance 500, Bruker, Billerica (MA), USA) in $CDCl_3$. The spectra were measured against the internal standard tetramethylsilane (TMS) and locked on the solvent signal of $CDCl_3$ at 7.26 ppm.

The average molecular weights and the polydispersity of the synthesized precursors were determined by gel permeation chromatography (GPC) in chloroform. The setup included a refractometer (Shodex RI-101, Showa Denko, Tokyo, Japan) and a dual viscosity/light scattering detector (T60A, Viskotec Corp., Tulare, USA). Chromatographic separation was conducted on two 300 mm x 8.0 mm SDV linear M columns with precolumns (PSS GmbH, Mainz, Germany).

The densities of the different phases were determined at 20 °C under atmospheric pressure by an oscillating u-tube (DMA 500; Anton Paar, Graz, Austria). As reference, the density of degassed water in Milli-Q quality was measured at 20 °C (ρ = 0.99820 g cm^{-3}). The solvent composition of the polymer phase was adjusted to the intended density and achieved by a linear regression of the measurements with different volume fractions φ of chloroform/toluene.

The methacrylate conversion during the PCL crosslinking was analyzed semi-quantitatively by FTIR spectroscopy (Nicolet 6700, Thermo Scientific, Waltham, USA) in attenuated total reflection (ATR) on a diamond-crystal using the C=C signal (=C—H out-of-plane bending vibration of vinyl group, 815 cm^{-1})

Table 1. Structural characterization of the synthesis products via GPC and ^{1}H-NMR spectroscopy.

Compound	M_n [a)] [g mol^{-1}]	M_w [a)] [g mol^{-1}]	PD	Arms [b)]
soCL-OH	12 300	14 700	1.2	3.4
soCL-IEMA	11 400	14 400	1.3	3.4

[a)] Determined by GPC; [b)] Determined by ^{1}H-NMR.

in relation to the signal intensity of non-crosslinked precursors in normalized spectra.

The thermal properties of precursors and microcapsules were characterized by differential scanning calorimetry (DSC) utilizing a Netzsch DSC 204 F1 (Selb, Germany). The calorimeter was purged with nitrogen during the heating/cooling cycles from −100 to 100 °C at heating and cooling rates of 10 K·min^{-1}. The data of the second heating run were used.

The microcapsule morphology and FITC-BSA encapsulation was investigated by light and fluorescence microscopy on a Leica DMI 6000 B (Wetzlar, Germany) using a digital camera DFC 310 FX.

2.5. Direct Cytotoxicity Tests with HEK Cells

HEK cells (5×10^5; InvivoGen, San Diego, USA) were cultured in 1 mL VLE-RPMI (Biochrom) in the presence of microcapsules (titration 0.016 to 1 mg mL^{-1}) for 24 h. The cell viability was assessed using FDA (25 µg·mL^{-1}) and PI (2 µg·mL^{-1}) staining. Each sample was evaluated at three different fields of view using a confocal laser scanning microscope (LSM 510 META, Zeiss, Oberkochen, Germany) with the AxioVision (Zeiss) image analysis software. Images were semi-quantitatively analyzed for the relative numbers of FDA and PI stained cells by ImageJ after image conversion to black/white images.

3. Results and Discussion

3.1. Synthesis and Characterization of Oligomeric Precursors

The non-functionalized, hydroxyl group-terminated oligomer was first synthesized by ring-opening polymerization (ROP) of CL. Using PERT as a tetravalent alcohol to initiate the tin(II) 2-ethylhexanoate catalyzed polymerization, 4-arm star shaped soCL was obtained. The number-average molecular weight M_n of this material was experimentally analyzed by GPC to be ≈12 kDa, which indicates some deviations from the M_n theoretically planned according to the reaction stoichiometry (8 kDa). This might be due to an incomplete initiation by PERT, resulting in a higher degree of polymerization. The polydispersity (PD) of the obtained oligomer was low (PD: 1.2) and in the typical range for the performed ROP (**Table 1**).

The average number of initiated arms was calculated from ^{1}H-NMR data (**Figure 2**). The signal at 4.12 ppm corresponds to the eight protons in α-position of the tetragonal center of the initiator (I2). The well separated signal at 3.65 ppm was assigned to the protons next to the hydroxyl endgroup of the last CL chain-segment (c6). A comparison of both signal intensities allowed determining the number of oligo(ϵ-caprolactone) arms to be 3.4 and therefore the amount of non-reacted initiator hydroxyl-groups as 0.6.

To enable later UV-induced crosslinking reactions, the termini of the synthesized oligomers were functionalized in a second reaction with methacrylate groups (IEMA) via a carbamate esterification reaction in dry DCM for 5 days.[34] The average molecular weight and the PD of the IEMA-functionalized oligomer (soCL-IEMA) well compare to non-functionalized precursors, suggesting negligible transesterification during the functionalization step (Table 1). From ^{1}H-NMR spectroscopy (Figure 2), the degree of functionalization was determined. Signals from the methacrylate endgroup appeared at 1.89 (M_{10}), 3.44 (M_3), 4.17 (M_4), 5.07 (M_2) and the two protons of the IEMA double-bond at 5.54 (M_9) and 6.07 ppm (M_8), respectively. The comparison of the signals of the double-bond with the initiator signal allowed to calculate the degree of functionalization, which was 3.4 and thus exactly matching the number of arms determined for the non-functionalized star-shaped soCL-OH precursor. Therefore, a complete conversion of the hydroxyl groups into methacrylate moieties was concluded. This result was also verified by the disappearance of the ^{1}H-NMR peak at 3.65 ppm, which was related to the hydroxyl-terminated chains. The structure was also verified by the ^{13}C-NMR data.

An additional qualitative analysis of the success of functionalization was performed by FTIR spectroscopy. After the IEMA functionalization, vibrational peaks appeared at 1637, 1530, and 815 cm^{-1} (**Figure 3**). These peaks could be assigned to vibrations of C═C, urethane, and C═C─H bonds, respectively, verifying a covalent attachment of the methacrylate group to the oligomer.

The thermal properties of the soCL materials were characterized by DSC (second heating run), revealing two melting transitions T_m at 51 and 54 °C, which were slightly shifted after IEMA-functionalization (**Table 2**). The presence of two melting peaks indicates the presence of two types of crystallite sizes, a crystal-to-crystal transition, or two coexisting crystalline structures, which is regularly found in oligo(ϵ-caprolactones).[35] From the melting enthalpy ΔH_m of both peaks, the weight crystallinity W_c was determined by using the theoretical enthalpy values for totally crystalline poly(ϵ-caprolactone).[36] The W_c of the soCL-OH was calculated to be 57%, whereas the crystallinity of the functionalized soCL-IEMA was slightly lower with values of 51%.

3.2. Microcapsule Templating and Crosslinking

Microcapsules with an aqueous core enclosed by a PCL network membrane were prepared by microfluidic templating, followed by crosslinking of the polymer shell. The aqueous core can serve as a reservoir, as should here be exemplified by a protein, and the PCL membrane acts as a diffusion barrier hindering the loss of the probe from the core compartment.

The inner aqueous phase (w_1) contained the fluorescent-labeled protein (FITC-BSA), Poloxamer as a stabilizing agent, and sodium chloride. The organic middle phase (o) was composed of 8.2 wt% solution of soCL-IEMA and Span 80 in a toluene/chloroform mixture. The w_1 and o phase were hydrodynamically focused in the microfluidic device (design and operation see Figure 1) by the outer continuous w_2 phase, an aqueous isotonic solution of PVA (5 wt.%). These conditions

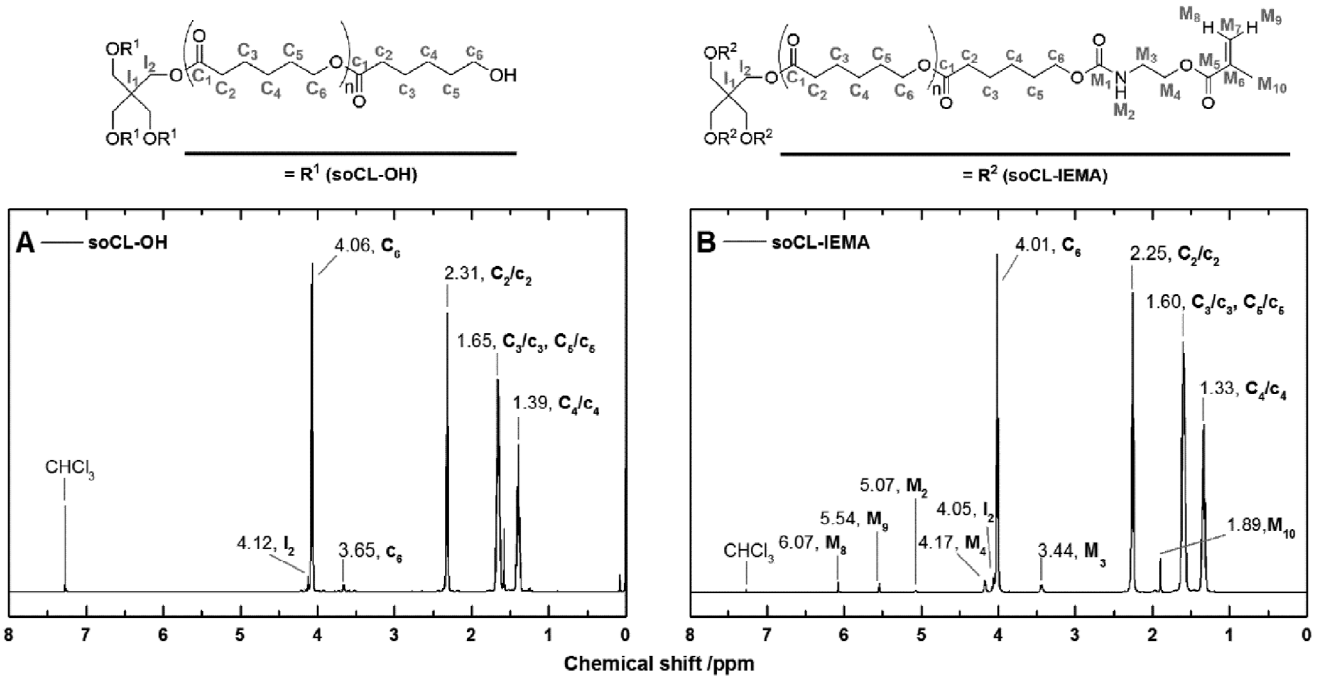

Figure 2. 500 MHz ^{1}H-NMR spectra and peak assignment of A) the hydroxyl- and B) 2-ethyl methacrylate-terminated oligo(ϵ-caprolactone) precursors in $CDCl_3$.

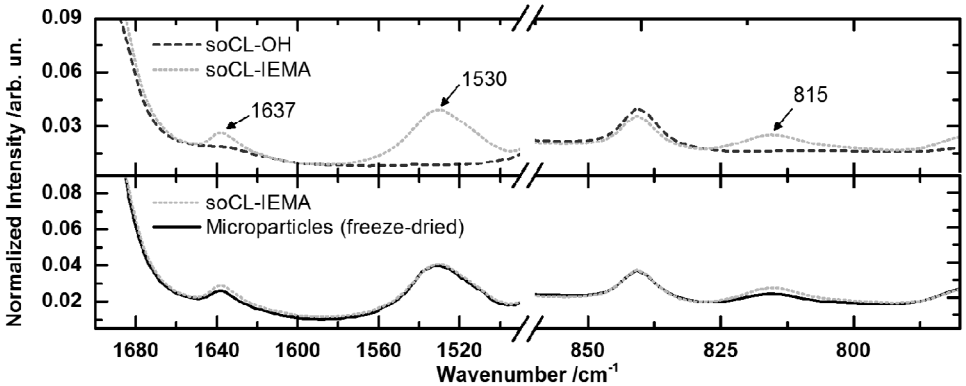

Figure 3. FTIR spectra of the oligomeric precursors soCL-OH/soCL-IEMA and freeze-dried microcapsules. The upper panel shows the successful coupling of IEMA as crosslinkable moiety. The lower panel shows the decrease of the C=C—H signal (815 cm^{-1}) due to partial methacrylate crosslinking during PCL network formation.

led to the desired well-controlled formation of double emulsion droplets (**Figure 4**) at the junction of the capillaries in the dripping mode. The frequency of droplet formation was ≈ 4000 Hz at flow-rates of $w_1/o/w_2$ = 0.4/2.0/14.0 mL·h^{-1}. The droplets were collected in an isotonic collection bath saturated with chloroform, which was sealed to avoid evaporation during the collection time. The formed droplets remained intact over > 1 h of collection. Importantly, a key step to obtain a stable

Table 2. Thermal properties of the oligomeric precursor and the microcapsule polymer network.

Compound	T_g [a)] [°C]	ΔC_p [J·(g K)$^{-1}$]	T_m [a)] [°C]	ΔH_m [J g^{-1}]	T_c [a)] [°C]	ΔH_c [J g^{-1}]	W_c [b)] [%]
soCL-OH	−65	0.068	51; 54	77.5	23	−73.3	57
soCL-IEMA	−52	0.147	49; 54	69.6	22	−64.0	51
Network microcapsule	−59	0.095	47; 51	60.4	19	−54.8	45

[a)] Averaged accuracy of the characterization method is ± 1 °C; [b)] Determined by DSC via $W_c = \Delta H_m/\Delta H_{m,0}\cdot 100\%$, theoretical 100% crystallinity at $\Delta H_{m,0}$ = 135.44 J g^{-1}.[36]

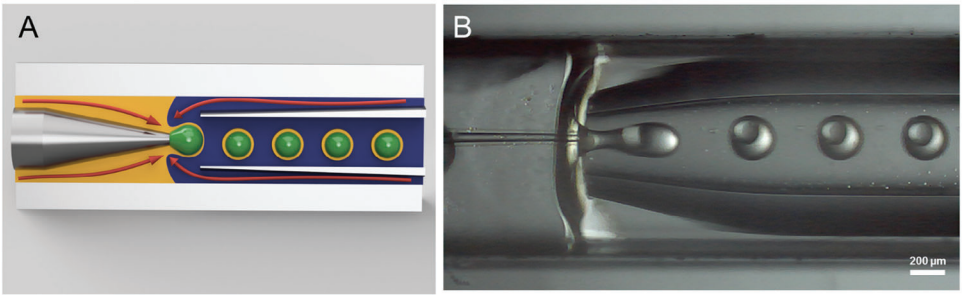

Figure 4. Double-emulsion droplet formation in the glass-capillary microfluidic device in the controlled dripping regime. A) Scheme. B) Experimental image as captured by high-speed microscopy.

and continuous double emulsion formation was to tailor the solvent composition of the organic phase. When the solvent composition was adjusted to match the density of the inner phase, an extensive floating of the aqueous core in the oil-droplet and a destabilization of the double emulsion structure during sample collection could be avoided, which also helped to achieve a homogeneous membrane thickness.

During photocrosslinking, methacrylate-functionalized soCL-IEMA precursors are expected to form a PCL network that should offer an enhanced integrity of the core-shell structure. Importantly, it was not possible to obtain stable particles with non-crosslinkable, i.e., linear and star-shaped hydroxyl terminated oligomers of molecular weights in the range of 10 000-30 000 g mol^{-1} in control experiments. Furthermore, experiments with bifunctional linear methacrylate terminated oligo(ϵ-caprolactone) of an average molecular weight of M_n = 10 000 g mol^{-1} did also not provide stable particle shells after crosslinking (data not shown). Only with the star-shaped soCL-IEMA it was possible to successfully prepare PCL network capsules in this study. Apparently, the successful crosslinking of oligo(ϵ-caprolactone) in the solution state (i.e., at a relatively low concentration and low proximity of methacrylate endgroups) was critically depending on the multivalency of the star-shaped precursor. This can be explained by the higher relative number of reactive groups (4-arm versus linear oCL-IEMA) and the star-shaped architecture of the precursor, which support the network formation in the particle shell.

In order to characterize the sizes of the formed particles, first the average diameters of the double-emulsion droplets were determined by light-microscopy measuring 100 droplets. In addition to the individual readings reported in **Figure 5**, the data were fitted with a normal distribution function $N(\mu, \sigma^2)$. Droplet diameters were determined to be 165 ± 4 µm for the inner diameter (ID) and 268 ± 10 µm for the outer diameter (OD) with a relative standard deviation (RSD) of 2% and 4%, respectively. Such narrow size distributions are typical for a successful microfluidic processing in the dripping regime and provided highly defined droplet templates for subsequent crosslinking of the shell. In general, the dimensions of the obtained droplet depend on the geometry of the microfluidic device (e.g., orifice diameters and distances of coaxial glass capillary assemblies), the viscosities of the different phases, and the flow conditions (e.g., flow rates and ratios of the different phases). While only one standardized condition was applied in this study, there is comprehensive literature

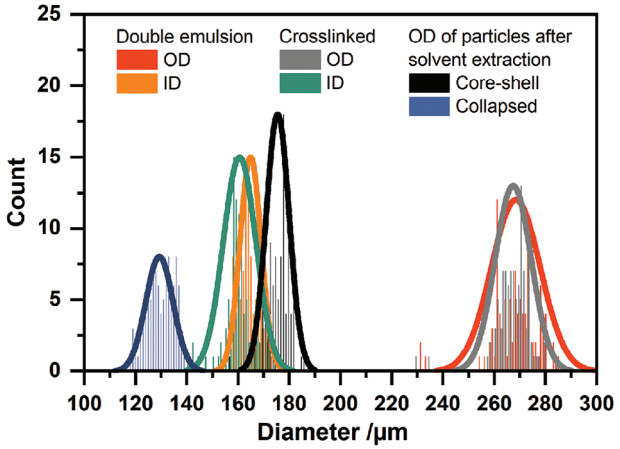

Figure 5. Size-distribution of the microcapsules after the different processing steps as determined by light microscopically: outer diameter (OD) and inner diameter (ID) of (i) emulsion droplets as prepared and (ii) solvent-containing particles after crosslinking as well as (iii) OD of particles after solvent extraction. Individual measurements (n = 100) are plotted as histogram with a bin size of 1 µm (bars), which were fitted as normal distribution (solid lines).

available illustrating the effect of parameter changes (e.g., flow rates) on droplet/particle sizes (e.g., ref. [37]).

Size characterization was furthermore conducted after the photocrosslinking of precursors in the organic middle phase. The sizes of the (still) solvent-containing particles with crosslinked shells remained practically unchanged with an ID of 161 ± 4 µm (RSD ≈ 4%) and an OD of 267 ± 7 µm (RSD ≈ 3%). This confirmed that the crosslinking step did not destabilize the core-shell structure, e.g. due to solvent loss by evaporation during irradiation. The solvent was subsequently extracted/evapoated in an isotonic aqueous hardening bath with an open air interface, followed by dialysis. After particle solidification, two particle fractions with different particle sizes were observed (Figure 5), which exhibited outer diameters of 129 ± 5 µm (RSD ≈ 4%) and 176 ± 5 µm (RSD ≈ 3%), respectively. The particles with a diameter of 176 ± 5 µm encapsulated an inner aqueous core of 161 ± 5 µm, i.e., the shell had an average thickness of 7.5 µm and thus was very thin as desired. However, the particle fraction with a diameter of 129 ± 5 µm exhibited a collapsed morphology, where the inner aqueous core was leaked during the solvent extraction.

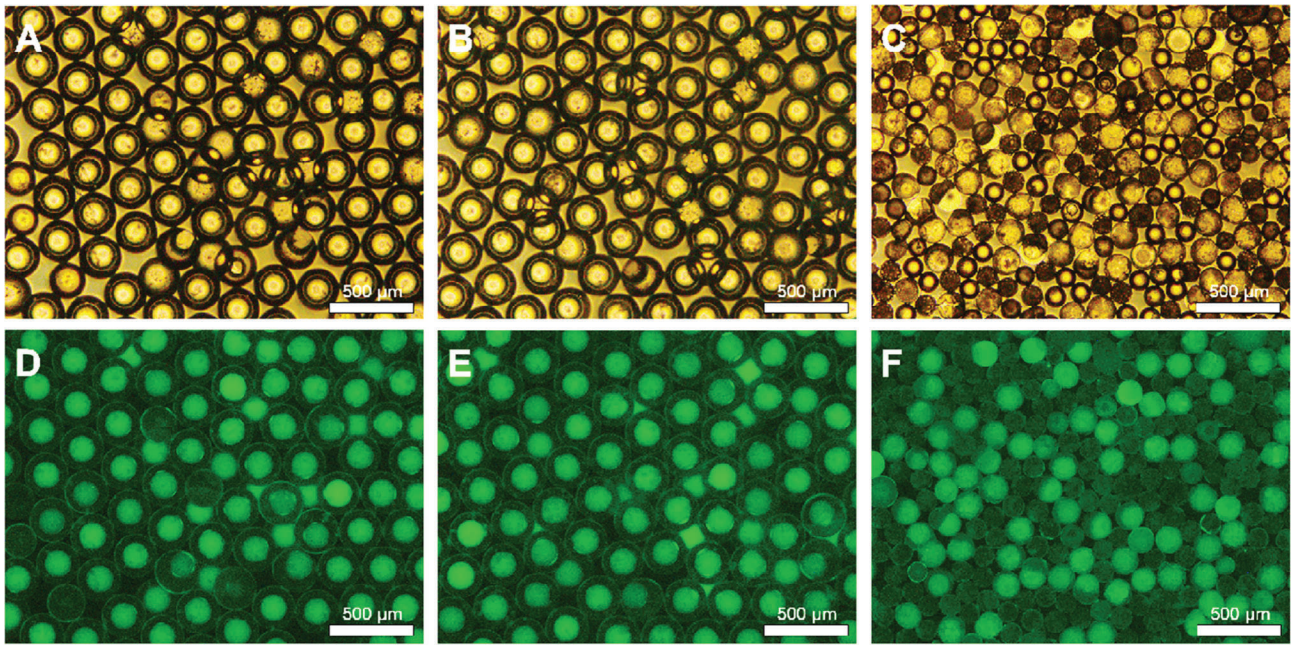

Figure 6. Light- and fluorescence-microscopic images of microparticles A,D) after microfluidic templating, B,E) after photo-polymerization, and C,F) after solvent extraction.

As the selected payload, FITC-BSA, is fluorescent, fluorescence microscopy allowed to conclude that the model component was successfully encapsulated by the PCL network shell (**Figure 6**). No changes of fluorescence intensities were observed after emulsification as well as after photo-polymerization, suggesting the stability of the probe. However, after particle solidification, differences in the fluorescence intensities of collapsed and core-shell particles were noted. The fluorescence intensity of the collapsed fraction of particles was substantially lower due to protein leakage, while the fluorescence intensity of the intact core-shell particles was nearly unchanged. The occurance of a fraction of collapsed particles may in principle be based on an insufficient network strength due to a low degree of crosslinking. In consequence, particles collapsed during the solvent extraction and deswelling of the poly(ϵ-caprolactone) network, which creates a mechanical stress along the membrane causing its rupture. The further collapse of the particles and leakage of the aqueous core would then be driven by interfacial tension.

One interesting application of such capsules may be in the field of drug delivery, where componds should be hosted inside particles and released subsequently, typically by diffusion through the membrane. The observed retention of FITC-BSA in intact capsules was expected given the relatively high molecular weight of BSA (66 kDa) compared to the much lower average chain segment length M_c that can be assumed for PCL networks made from ≈12 kDa 4-arm precursors. In literature, an M_c as low as 2.3 kDa was determined for PCL networks from 8 kDa 4-arm precursors,[21] which supports the prevention of FITC-BSA diffusion through the PCL network membrane. If a functional cut-off of such capsule membranes should be determined in future studies, the encapsulation of dextrans of different molecular weights and an analysis of diffusion coefficients might be applied.[38]

In a next step, particle aliquots were freeze-dried and investigated by ATR-FTIR to semi-quantitatively study the conversion of methacrylate endgroups after UV treatment. This analysis was based on the relative change of the methacrylate vibration signal at 815 cm^{-1} after photo-polymerization, where a low conversion of ≈ 40 mol% was determined. Due to the low molecular weight of the oligomer and an assumed absence of a major portion of physical netpoints by chain entanglements (due to crosslinking in a solvent-containing, i.e., diluted state), this low conversion (i.e., limited number of covalent netpoints) is a likely reason for the appearance of some collapsed particles. An increased UV curing time or altered light exposure conditions may possibly enhance the particle fraction with stable core-shell morphology. Additionally, in the future, precursors with more reactive functionalities, e.g. of comb-like grafted architecture may be studied. Given the differences in sizes and fluorescence intensity of intact and damaged (core-lacking) particles, a post-production separation should be possible, e.g. by FACS technology with sufficiently large channels.[39]

After photocrosslinking, a decrease of melting temperatures T_m and enthalpies ΔH_m of the PCL network capsules was observed compared to the precursors (Table 2 and **Figure 7**). This can be explained by a reduction of crystal size and crystallinity, which was caused by the newly formed polymethacrylate linkers, evoking discontinuities inside the PCL network and reducing the PCL chain mobility. Compared to high molecular weight PCL or highly crosslinked PCL-based networks with typically single melting peaks,[40] here again two T_m's were found. This supports an only partial crosslinking of the available methacrylate moieties with a preserved capability of the segments to organize into crystallites of different sizes.

Beside the influence of the crosslinking density on the particle stability, the semi-crystalline character of the particle shell

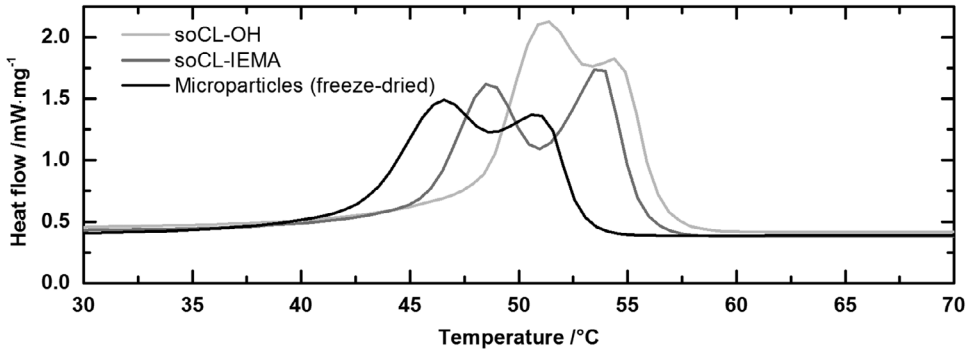

Figure 7. Dry state DSC curves of the melting region of the oligomeric precursors and the freeze-dried microcapsules.

material (W_c = 45%) might theoretically also affect the integrity of the particle membrane. Possibly, the crystallization of the shell could introduce additional mechanical stress inside the particle shell by volume contraction, which would have a destabilizing effect. A link of such phenomena to the specific dimension of the polymer network material can be expected. They may become particularly relevant for small particles (highly curved interface), particles with shell thicknesses in the range of only a few micrometers or less, and for particles with a high shell volume loss during solvent extraction and evaporation. Thus, when further

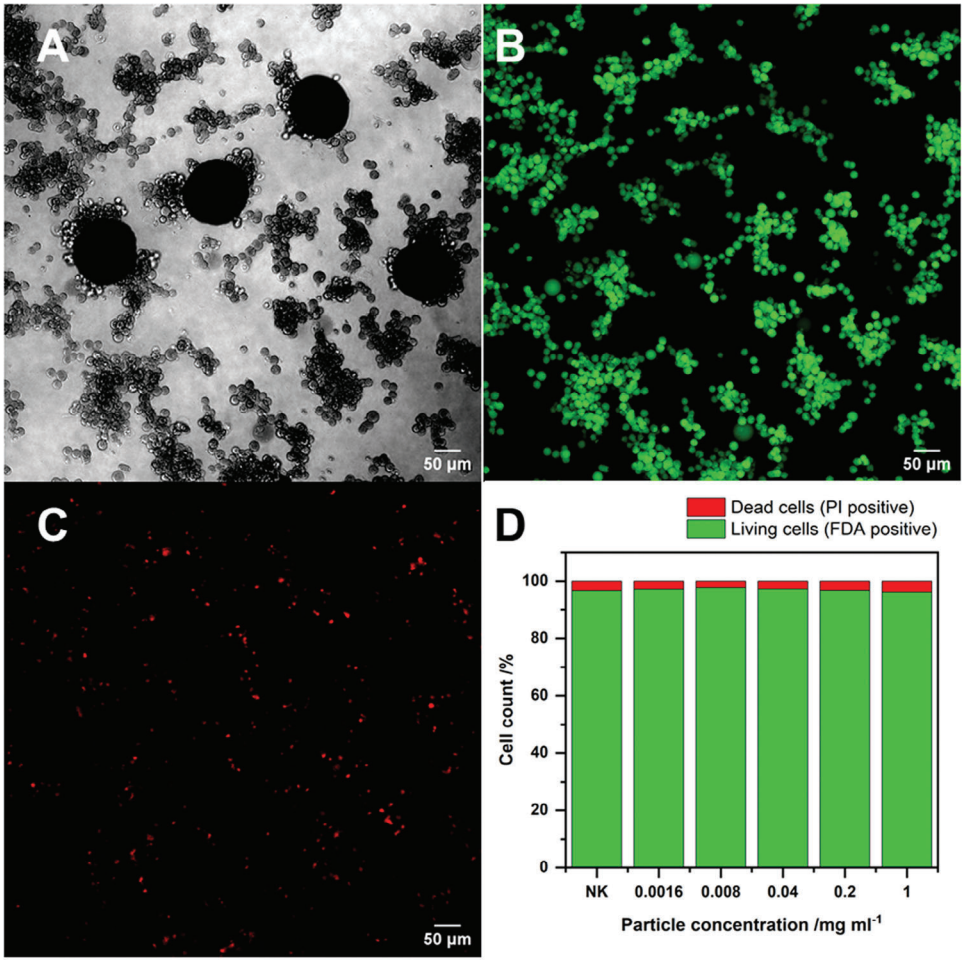

Figure 8. Evaluation of cell toxic effects by direct exposure of HEK cells to PCL network particles suspended in the cell culture medium. A–C) Microscopic analysis of FDA/PI stained HEK-cells after incubation with microcapsule suspension of 1 mg mL^{-1} for 24 h. (A) Bright-field image show HEK-cells in direct contact with microcapsules (large circular objects covered with cells). (B) FDA-positive living cells are shown. (C) PI-positive dead cells are shown. D) Estimated portion of live and dead cells based on image analysis for titration experiment with increasing concentrations of suspended particles in the cell culture (NK: negative control).

miniturizing polymer network materials synthesized in solution state, particular attention should be paid to forces originating from network contraction.

3.3. Cell Viability Upon Particle Contact

PCL is a material used in biomedical products, for which biocompatibility is an important requirement. In this respect, it always relevant to consider the processing history of materials. For instance, the chemical functionalization and further processing of PCL was performed in this study in presence of cytotoxic solvents and catalysts. Therefore, an investigation of cytotoxicity should be included in this study.

In order to determine possible cytotoxic effects, HEK cells were cultivated in direct contact with the microcapsules (direct cytotoxicity tests). The images (**Figure** 8A) indicated that HEK cells can directly interact with particles. Thus, in addition to potential long-distance effects by extractable compounds, a potential material cytotoxicity should be detectable particularly for cells in the proximity of the microcapsules. Initially, titration experiments with increasing concentrations of particle suspensions from 0.016 to 1 mg mL^{-1} were conducted. The viability of these adherent cells was microscopically studied by the FDA-PI live-dead staining conducted after 24 h of incubation, without relevant differences between the different experimental conditions. Therefore, only the images for the highest particle concentration (1 mg mL^{-1}) are displayed in Figure 8, showing a high viability as indicated by the high fluorescence signal intensity of FDA (Figure 8B). The presence of dead cells could be determined by PI staining, which was minimal (Figure 8C) and comparable to control experiments without microcapsules. When further comparing Figure 8A,C, it is also obvious that there was no accumulation of dead cells around the particles (large spherical objects in Panel A). Via image analysis, the overall portion of dead cells was estimated to be <5% (Figure 8D).

4. Conclusion

In this study, PCL network-based core-shell microparticles were prepared by a microfluidic double-emulsion approach. The particle templates were obtained with well-defined sizes, narrow size distributions, and a large aqueous compartment. The photo-crosslinking did not affect the particle size and morphology. While the preparation of PCL network particles under photoinitiator-free conditions was possible as planned and led to particles with the desired core shell-morphology after solvent extraction, there was also a fraction of collapsed particles arising after this final processing step. FTIR investigations of freeze-dried particles showed a relatively low conversion of the methacrylate endgroups despite exposure to an intense light source for crosslinking, which suggests insufficient network strength as the major reason for the collapse of a certain fraction of particles.

A high protein loading capacity was found for the successfully formed core-shell particles. The microcapsules did not affect the cell viability of a human-derived model cell-line in a first set of experiments, suggesting that cytocompatibility may be established and documented in more comprehensive biological studies in the future.

Based on the data of this pilot study, concepts to increase the crosslink density of the microcapsule wall and thus to potentially enhance the particle stability might be explored in the future, e.g. by extended photo-polymerization times or by the utilization of oligomers with a higher number of reactive methacrylate endgroups (6-arm star-shaped or comb-like oligomers). Furthermore, leakage profiles of the payload, stability of the payload during storage, or particle degradation kinetics could be studied depending on the desired specific application of PCL network capsules.

Acknowledgements

The authors thank Angelika Ritschel for performing the cytotoxicity tests. Linus Wolf, Xun Xu, and Weiwei Wang were acknowledged for help with image analysis. Funding of the Helmholtz Association through program-oriented funding was acknowledged.

Conflict of Interest

The authors declare no conflict of interest.

Author Contributions

F.S. contributed in conceptualization, methodology, formal analysis, investigation, and writing—original draft, review, and editing. T.R. contributed in conceptualization, methodology, formal analysis, and writing—review and editing. A.L. contributed in conceptualization, supervision, funding acquisition, and writing—review and editing. C.W. contributed in conceptualization, resources, data curation, supervision, project administration, funding acquisition, and writing—original draft, review and editing.

Data Availability Statement

The data that support the findings of this study are available from the corresponding author upon reasonable request

Keywords

biocompatibility, microfluidics, photocrosslinking, poly(ϵ-caprolactone), polymer networks

Received: June 30, 2023
Revised: December 25, 2023
Published online: January 18, 2024

[1] Y. Gu, J. Zhao, J. A. Johnson, *Angew. Chem., Int. Ed.* **2020**, *59*, 5022.
[2] J. Li, D. J. Mooney, *Nat. Rev. Mater.* **2016**, *1*, 16071.
[3] D. Jiao, Q. L. Zhu, C. Y. Li, Q. Zheng, Z. L. Wu, *Acc. Chem. Res.* **2022**, *55*, 1533.
[4] M. Li, A. Pal, A. Aghakhani, A. Pena-Francesch, M. Sitti, *Nat. Rev. Mater.* **2022**, *7*, 235.
[5] X. Zhang, J. Xiang, Y. Hong, L. Shen, *Macromol. Rapid Commun.* **2022**, *43*, 2200075.
[6] X. Lin, X. Zhao, C. Xu, L. Wang, Y. Xia, *J. Polym. Sci.* **2022**, *60*, 2525.
[7] X. Zhao, X. Chen, H. Yuk, S. Lin, X. Liu, G. Parada, *Chem. Rev.* **2021**, *121*, 4309.

[8] X. Liu, J. Wu, K. Qiao, G. Liu, Z. Wang, T. Lu, Z. Suo, J. Hu, *Nat. Commun.* **2022**, *13*, 1622.
[9] A. C. Weems, A. Easley, S. R. Roach, D. J. Maitland, *ACS Appl. Bio Mater.* **2019**, *2*, 454.
[10] A. U. Vakil, N. M. Petryk, E. Shepherd, H. T. Beaman, P. S. Ganesh, K. S. Dong, M. B. B. Monroe, *ACS Appl. Bio Mater.* **2021**, *4*, 6769.
[11] G. S. Offeddu, E. Axpe, B. A. C. Harley, M. L. Oyen, *AIP Adv.* **2018**, *8*, 105006.
[12] P. Nicolella, D. Lauxen, M. Ahmadi, S. Seiffert, *Macromol. Chem. Phys.* **2021**, *222*, 2100076.
[13] N. Tsutsumi, Y. Kono, M. Oya, W. Sakai, M. Nagata, *CLEAN—Soil, Air, Water* **2008**, *36*, 682.
[14] G. X. De Hoe, M. T. Zumstein, B. J. Tiegs, J. P. Brutman, K. Mcneill, M. Sander, G. W. Coates, M. A. Hillmyer, *J. Am. Chem. Soc.* **2018**, *140*, 963.
[15] W. Ussama, M. Shibata, *Polymer* **2022**, *244*, 124668.
[16] Chen, D. R., J. Z. Bei, S. G. Wang, *Polym. Degrad. Stab.* **2000**, *67*, 455.
[17] D. P. Go, D. J. E. Harvie, N. Tirtaatmadja, S. L. Gras, A. J. O'Connor, *Particle Particle Syst. Character.* **2014**, *31*, 685.
[18] F.-L. Zhou, P. L. Hubbard Cristinacce, S. J. Eichhorn, G. J. M. Parker, *Aerosol Sci. Technol.* **2016**, *50*, 1201.
[19] R. F. Storey, S. C. Warren, C. J. Allison, J. S. Wiggins, A. D. Puckett, *Polymer* **1993**, *34*, 4365.
[20] F. Friess, A. Lendlein, C. Wischke, *MRS Online Proc. Lib.* **2013**, *1569*, 173.
[21] F. Friess, U. Nöchel, A. Lendlein, C. Wischke, *Adv. Healthcare Mater.* **2014**, *3*, 1986.
[22] I. Sedov, T. Magsumov, A. Abdullin, E. Yarko, T. Mukhametzyanov, A. Klimovitsky, C. Schick, *Polymers* **2018**, *10*, 902.
[23] Y. He, C. J. Tuck, E. Prina, S. Kilsby, S. D. R. Christie, S. Edmondson, R. J. M. Hague, F. R. A. J. Rose, R. D. Wildman, *J. Biomed. Mater. Res., Part B* **2017**, *105*, 1645.
[24] E. Zant, D. W. Grijpma, *Acta Biomater.* **2016**, *31*, 80.
[25] Friess, F., A. Lendlein, C. Wischke, *Polym. Adv. Technol.* **2014**, *25*, 1285.
[26] Wischke, C., *Int. J. Pharm.* **2020**, *584*, 119401.
[27] I. B. Bekard, P. Asimakis, J. Bertolini, D. E. Dunstan, *Biopolymers* **2011**, *95*, 733.
[28] G. Ma, *J. Controlled Release* **2014**, *193*, 324.
[29] H. J. Kwon, S. Kim, S. Kim, J. H. Kim, G. Lim, *BioChip J.* **2017**, *11*, 214.
[30] A. Forigua, A. Dalili, R. Kirsch, S. M. Willerth, K. S. Elvira, *ACS Appl. Polym. Mater.* **2022**, *4*, 7004.
[31] C.-H. Yang, K.-S. Huang, Y.-S. Lin, K. Lu, C.-C. Tzeng, E.-C. Wang, C.-H. Lin, W.-Y. Hsu, J.-Y. Chang, *Lab Chip* **2009**, *9*, 961.
[32] M. Duran, A. Serrano, A. Nikulin, J. L. Dauvergne, L. Derzsi, E. P. del Barrio, *Mater. Des.* **2022**, *223*, 111230.
[33] G. Wei, L. F. Lu, W. Y. Lu, *Int. J. Pharm.* **2007**, *338*, 125.
[34] M. Balk, M. Behl, U. Nöchel, A. Lendlein, *Macromol. Mater. Eng.* **2012**, *297*, 1184.
[35] K. Takizawa, C. Tang, C. J. Hawker, *J. Am. Chem. Soc.* **2008**, *130*, 1718.
[36] V. Crescenzi, G. Manzini, G. Calzolari, C. Borri, *Eur. Polym. J.* **1972**, *8*, 449.
[37] G. T. Vladisavljević, H. C. Shum, D. A. Weitz, in *Control over the Shell Thickness of Core/Shell Drops in Three-Phase Glass Capillary Devices in UK Colloids*, Springer, Berlin, Heidelberg **2012**.
[38] F. Cellesi, N. Tirelli, J. A. Hubbell, *Biomaterials* **2004**, *25*, 5115.
[39] S. Kannan, M. Miyamoto, B. L. Lin, R. Zhu, S. Murphy, D. A. Kass, P. Andersen, C. Kwon, *Circ. Res.* **2019**, *125*, 567.
[40] L. Cai, S. Wang, *Polymer* **2010**, *51*, 164.